Emission of ^{3}He and ^{4}He in reactions of 70- and 160-MeV $\pi^\pm$ mesons with Ag

S. B. Kaufman, B. D. Wilkins, and D. J. Henderson
Chemistry Division, Argonne National Laboratory, Argonne, Illinois 60439

R. E. L. Green and R. G. Korteling
Department of Chemistry, Simon Fraser University, Burnaby, British Columbia, Canada V5A 1S6

G. W. Butler
Isotope and Nuclear Chemistry Division, Los Alamos National Laboratory, Los Alamos, New Mexico 87545
(Received 17 May 1985)

Energy spectra of ^{3}He and ^{4}He emitted in the reactions of 70- and 160-MeV $\pi^\pm$ mesons with Ag were measured at seven angles with respect to the beam, from 30° to 160°. The spectra are similar in both shape and magnitude to the corresponding spectra observed at an angle of 90° in the reactions of 300—480 MeV protons with the same target. The spectra from $\pi^\pm$ reactions are nearly independent of angle, in contrast to the strong angular dependence of the high-energy particles observed in reactions of protons and other projectiles. These observations, as well as the π^+/π^- ratios for the yields of ^{3}He and ^{4}He, are interpreted in terms of pion absorption and subsequent interactions of the resulting fast nucleons leading to fragment emission.

I. INTRODUCTION

A characteristic feature of nuclear reactions at intermediate to high energies (i.e., above compound-nucleus energies) is the emission of energetic particles in the continuum.[1] The energy spectra and angular distributions of these energetic particles distinguish them from evaporation particles emitted in the statistical deexcitation of a fully equilibrated residual nucleus, and suggest that their origin is in the early stages of the reaction. The energy spectra above the evaporation region are typically of the form $\exp(-E/T)$ in the kinetic energy E, with the parameter T a strong function of the angle of emission. At forward angles T is much larger than the equilibrium nuclear temperatures expected if the available excitation energy were distributed over the entire nucleus, and T decreases with increasing angle toward the thermal value. Thus, the angular distributions of these energetic particles are characteristically forward peaked in the laboratory, in contrast to the nearly isotropic emission pattern of the evaporative component of the spectrum. Examples of these so-called preequilibrium particles are the emission of isotopes of H and He in reactions of 90 MeV protons,[2] 80 MeV deuterons,[3] and 140 MeV alpha particles[4] with a number of targets, and fragments of $Z=2$—12 in reactions of 210—480 MeV protons with Ag.[5–7]

A number of different models have been applied in order to account for the emission of these nonevaporative particles. A direct knockout model, in which the projectile strikes a cluster of nucleons moving with high momentum, was used to fit the energy spectra at different angles of fragments observed in intermediate energy proton-induced reactions.[8,9] Statistical models assuming isotropic emission of fragments from a moving source can account for these data also, provided the source velocity is allowed to be a function of the fragment velocity in the moving frame.[7] Intermediate between these extremes are final-state interaction models, such as pickup[9–11] and coalescence[12,13] models.

One experimental approach which may help to distinguish between different models or at least place constraints on them is to compare the properties of fragments emitted in reactions of different projectiles. An example is the comparison of the ^{4}He spectra for electron-induced[14–16] and proton-induced reactions near 100 MeV projectile energy. The energy spectra are similar in shape and in their dependence on emission angle, but the cross sections for the (e,α) reactions are 10^{-4} to 10^{-5} as large as those for (p,α). This is of the order of the cross section ratio expected for a single scattering of the projectile from a nucleon,[17] and suggested a mechanism in which there is one primary scattering, after which the recoiling nucleon may form the observed fragment via final-state interactions. This is distinguished from the usual coalescence model of relativistic heavy-ion reactions in which a nucleonic cascade results from multiple scattering of the projectile.

The use of pions as projectiles to study energetic fragment emission can provide some unique properties in comparison with the more usual projectiles. Pion absorption inside the nucleus can transfer considerable energy without transferring much momentum, in contrast to projectiles whose only interaction is nucleon scattering. For pion energies below about 100 MeV absorption is the dominant reaction channel. The availability of both positive and negative pions allows one to study isospin effects in reaction mechanisms; for example, π^+ absorption on a quasideuteron results in two protons, while π^- absorption yields two neutrons. Thus, the importance of final-state interactions in charged-particle emission may be probed by comparing the yields from the two charge states.

There is little data available on light fragment emission

induced by energetic pions. Amann *et al.*[18] measured the high-energy ($E > 50$ MeV) spectra of ^{3}He and ^{4}He emitted at 90° from the reactions of 235-MeV π^+ mesons with targets of Mg, Ni, and Ag, and concluded that their cross sections were consistent with a nucleon-pickup mechanism. Doron *et al.*[19] measured ^{4}He spectra in the low-energy evaporation region, and also at a single angle, 90°, for 70 MeV positive and negative pions interacting with targets of C, Al, Ni, and Ag. Energy spectra of light fragments emitted from different nuclei following absorption of stopped negative pions have also been measured in several experiments.[20] In order to obtain more extensive data on pion-induced light-fragment emission, especially at a range of emission angles, we have measured the energy spectra as a function of emission angle for ^{3}He and ^{4}He resulting from the reactions of positive and negative pions with Ag at two incident energies, 70 and 160 MeV.

II. EXPERIMENTAL

The experiment was performed using a 70-cm diameter evacuated scatter chamber located at the low-energy pion channel of the Clinton P. Anderson Meson Physics Facility (LAMPF). Beams of both positive and negative pions with energies of 70 and 160 MeV were focused to a spot at the target which was approximately circular, with about 90% of the intensity within a radius of 1.5 cm. The target was a metallic silver foil, 10 cm × 10 cm and 25 mg/cm^2 thick, mounted at an angle of 55° to the beam. Fragments emitted from the target were detected by ten ΔE-E silicon detector telescopes positioned at angles between 30° and 160° to the beam, and all in the same plane, as shown schematically in Fig. 1. Pairs of telescopes were placed symmetrically on opposite sides of the beam at 30°, 90°, and 160°, while single telescopes were at 50°, 70°, 110°, and 130°. The 30° and 160° telescopes were at a distance of 30 cm from the target, in order to keep them out of the halo around the beam, while the other telescopes were 17 cm from the target. With this arrangement of multiple detectors, data were collected simultaneously at all angles, eliminating normalization measurements for the angular distributions.

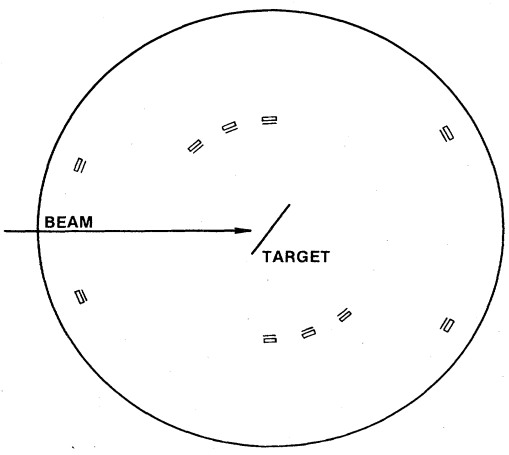

FIG. 1. Schematic diagram of the arrangement of detector telescopes around the target.

The E detector in each telescope was 2000 μm thick, and the ΔE detectors were 130—140 μm thick in most cases. These thicknesses permitted the identification of ^{3}He fragments over the energy range 13—66 MeV and ^{4}He from 15—74 MeV. The telescope at an angle of 50° had a ΔE detector thickness of 50 μm, allowing detection of fragments down to about 9 MeV. The discriminator thresholds were set low enough to detect all He ions within these energy limits, but high enough to cut out most of the energetic protons, deuterons, and tritons, since the E-detector thickness was sufficient to stop only a small fraction of the energy spectrum of the latter particles. A third detector behind the E detector was used to veto particles which did not stop in the E detector. The energy response of each detector was determined using radioactive alpha-particle sources and a precision pulse generator. These calibrations were checked periodically during the course of the experiment.

Signals from the detectors were processed with conventional preamplifiers, amplifiers, and discriminators. A coincidence between the ΔE and the E detector of each telescope defined a valid event. The ten individual coincidence outputs went to a fan-in circuit, the output of which generated the master trigger which enabled the data acquisition process. The signals from the linear amplifiers were digitized by CAMAC ADC's to provide the energy deposited in each detector.

Upon receipt of an event trigger a computer interrupt was generated, and the ADC's were read into a data buffer, the contents of which were written onto magnetic tape when the buffer was filled. The number of counts for each telescope was recorded by CAMAC scalers, which were read out periodically and written to magnetic tape during each run. The ratio of the number of recorded events to the scaler count for each detector measured the total effective live time. Because the time required to read the data for each event was about 1.8 msec, longer than the duration of a single macropulse of the accelerator, at most one event per macropulse could be recorded. The live time measured in this way varied from 90% at the highest data rates (15 counts/sec) to 99% at the lowest rate (1 count/sec). At these relatively low singles rates, pileup effects and other sources of dead time were negligible.

The relative beam intensity during a run was monitored by the beam-on-target signal from the accelerator, and also by the count rate in a plastic scintillator telescope which viewed the pion beam at the exit window of the scatter chamber and recorded decay muons. The absolute intensity for each beam and energy was determined by activation of thin aluminum foils placed at the entrance and exit windows of the scatter chamber during a single run. The induced ^{18}F activity was measured by counting the annihilation radiation, and the total number of pions passing through the foils calculated from the experimental cross sections.[21] The intensity measured at each window was then corrected for the decay of pions in the beam traveling from the entrance window to the target and from the target to the exit window. The two independent

measurements agreed within the statistics of the data. Average intensities varied from 1×10^7 pions/sec (70 MeV π^-) to 5×10^7 pions/sec (160 MeV π^+). A data run was taken for each beam with an empty target frame replacing the target and frame, in order to subtract the target-out background for each telescope.

The off-line analysis of the data was done in three stages. First, a particle-identifier (PI) value, proportional to the fragment MZ^2, was calculated for each event, using an algorithm based on an integration of the Bethe-Bloch stopping power equation.[22] An example of a PI spectrum for a typical detector is shown in Fig. 2, illustrating the separation of ^{3}He and ^{4}He. The points show the target-in data, while the histogram (binned in five-channel intervals) indicates the PI spectrum for the corresponding target-out run, normalized to the same number of incident pions. It is clear from this comparison that events outside the peaks due to the He isotopes do not originate from the target, but rather are due to another source associated with the beam, such as the beam halo or the neutron background near the beam. An exception was found for the pair of telescopes positioned at 160°, for which a significant contribution from ^{3}He and ^{4}He fragments was observed in the target-out data. These presumably originated in a source in or near the exit window of the scatter chamber, downstream from the target, which these telescopes could view. Subtraction of the target-out spectrum thus resulted in larger uncertainties in the 160° spectra than at other angles.

In the second stage of the data analysis, windows corresponding to ^{3}He and ^{4}He were set on the PI spectra for each detector, and energy spectra for the two isotopes were accumulated. In the final step, the target-out energy spectra were smoothed to reduce statistical fluctuations, normalized to the same number of incident pions as the target-in spectra and subtracted from the latter. The resulting spectra, in terms of net counts, were converted to differential cross sections for each telescope, $d^2\sigma/d\Omega\,dE$. The latter were then corrected for energy loss in the target, assuming all fragments originated at the center of the target. This correction decreases with increasing fragment energy; for ^{4}He fragments emitted normal to the target surface the correction is 2.1 MeV for an observed fragment energy of 15 MeV, decreasing to 0.8 MeV at 70 MeV. The energy-loss correction was greatest for the telescope at 30° for which the detected fragments were emitted at an angle of 25° with respect to the target, being 2.3 times as large as for perpendicular emission. Although the assumption that all fragments originate in the center of the target does not correct for the dispersion caused by the finite target thickness, the spectra are sufficiently smooth that the shapes are not appreciably affected. Comparison of the corrected spectra for the three pairs of telescopes at the same angles on opposite sides of the beam revealed no systematic differences in shape or magnitude, thus serving as a check on the centering of the beam on the target and the energy loss correction. The final spectra at these angles were calculated as the weighted average of the two independent measurements.

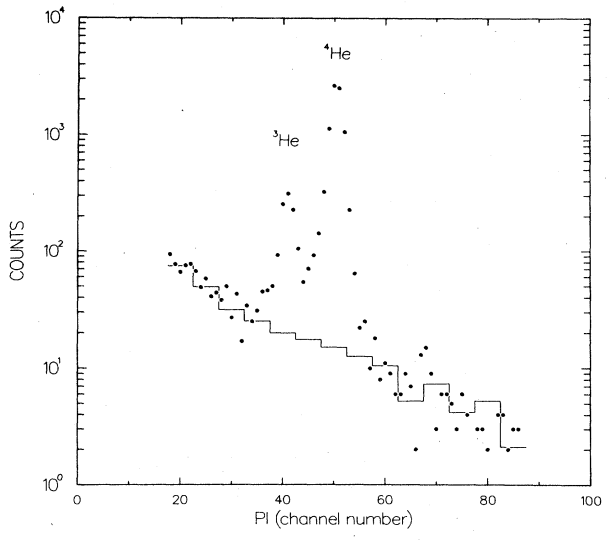

FIG. 2. Particle identifier (PI) spectrum for a typical telescope. The target-in data are shown by the points, and the target-out spectrum, normalized to the same number of incident pions, is shown by the histogram.

The statistical errors were obtained in terms of the number of observed counts in each energy bin in the target-in and target-out spectra. An additional 10% uncertainty was assumed for the relative normalization of the target-out data in the subtraction. This is a significant source of error only for the pair of telescopes at 160°, for which the correction was as large as 50% for ^{3}He and 30% for ^{4}He at the higher energies. The main uncertainty in the absolute scale of cross section lies in the values of the monitor cross sections for forming ^{18}F from aluminum, which are estimated[21] to have a precision of 5%.

III. RESULTS

The energy spectra of ^{3}He and ^{4}He from the 160-MeV π^+ bombardment are shown in Figs. 3 and 4 as a function of the laboratory angle. The spectra resulting from negative pions of the same energy, and from positive and negative pions of 70 MeV, are quite similar in shape to those shown, but differ in magnitude; the differences are discussed below. Figure 3 shows the ^{3}He differential cross sections (corrected for the average energy loss in the target, as discussed in the previous section) at each laboratory angle, with the different spectra offset by successive factors of 10 for ease of comparison. The data were binned into 5-MeV intervals centered at energies from 20 to 60 MeV; the 50° spectrum has an additional data point at 15 MeV, because the thin ΔE detector in that telescope resulted in a lower cutoff energy. These spectra all have a smooth energy dependence, very well approximated by a simple exponential falloff with fragment energy, $\exp(-E/T)$, as has been typically observed for these fragments emitted in other medium-energy reactions. However, there is little variation of the spectral shape with emission angle, in contrast to the angular dependence observed with other projectiles.[2–6,14–16]

In order to illustrate the differences between the pion-induced fragment spectra and those from proton-induced

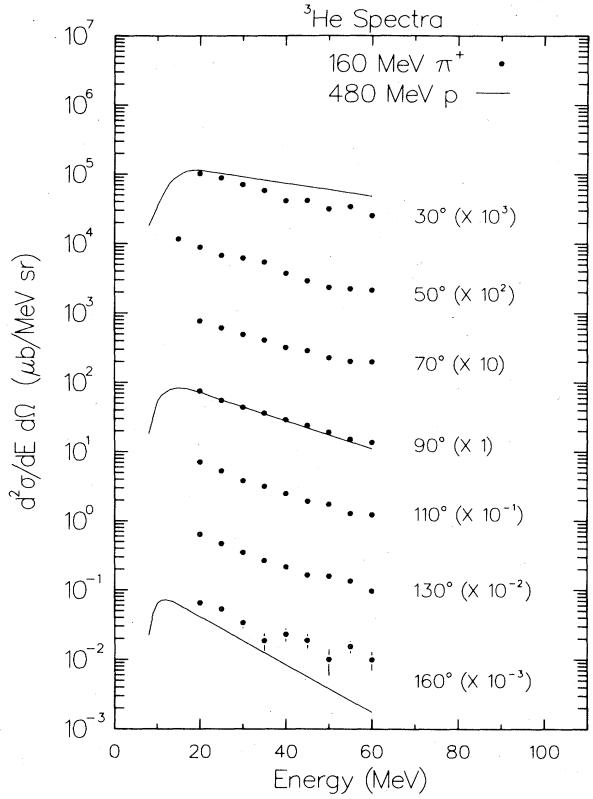

FIG. 3. Energy spectra of ^{3}He fragments as a function of emission angle for 160-MeV π^+ interacting with Ag. The smooth curves show the ^{3}He spectra for 480-MeV proton interactions with Ag (from Ref. 6).

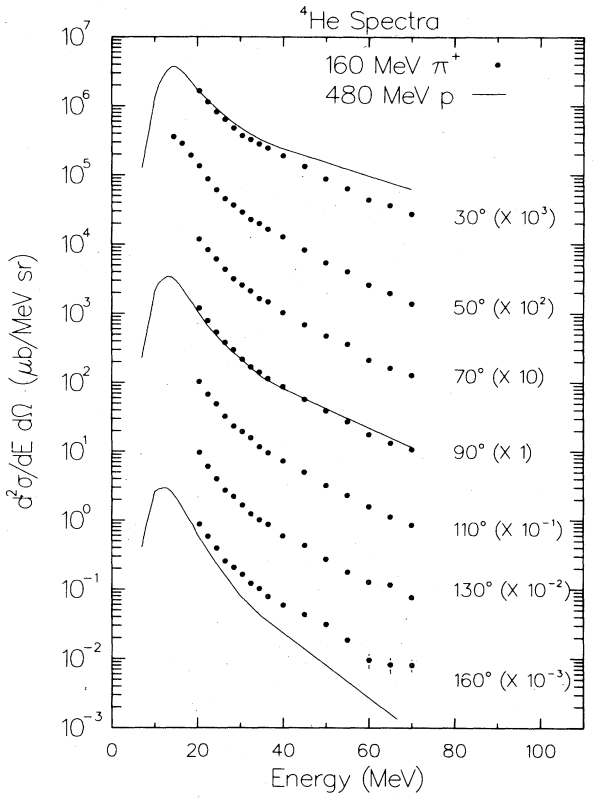

FIG. 4. Energy spectra of ^{4}He fragments as a function of emission angle for 160-MeV π^+ interacting with Ag. The smooth curves show the ^{4}He spectra for 480-MeV proton interactions with Ag (from Ref. 6).

reactions we show by smooth curves the ^{3}He energy spectra at angles of 20°, 90°, and 160° observed in the reactions of 480-MeV protons with silver.[6] At 90° the spectra for the two different projectiles not only have the same shape but fortuitously have the same absolute cross sections, thus making the comparisons at the other angles straightforward. At the forward angle (neglecting the difference between 20° and 30°) the cross section is larger for incident protons, and the slope of the exponential part of the spectrum is less steep. At the backward angle these relationships are reversed, with smaller cross sections and a steeper slope for the proton-induced reaction. The result of these differences is a much stronger variation with angle for the fragment spectra from incident protons than pions. The slope parameter, T, for the ^{3}He spectra from 160-MeV pions decreases from $T=28$ MeV at 30° to $T=18$ MeV at 160°; for 480-MeV protons the slopes decrease from 48 to 12 MeV with increasing angle. At 70 MeV incident pion energy the slopes of the ^{3}He spectra are almost independent of emission angle, with a mean value of $T=22$ MeV.

The same comparisons for ^{4}He fragments are shown in Fig. 4, again for 160-MeV π^+ and 480-MeV protons. The data for the pion-induced reactions are binned in 2-MeV intervals between 20 and 36 MeV and in 5-MeV intervals from 40 to 70 MeV. (At 50° the telescope was sensitive down to 14 MeV.) The spectra are smooth and exhibit two components, a low-energy one arising from statistical evaporation superimposed on the high-energy preequilibrium spectrum. The smooth curves are the corresponding spectra for 480-MeV proton reactions with silver,[6] and show the Coulomb peak in the low-energy region which was not accessible in the present experiment. The ^{4}He spectra at 90° measured by Doron *et al.*[19] in the low-energy region at a pion energy of 70 MeV also show the Coulomb peak, and are in good agreement with the present data where they overlap. As is the case for ^{3}He, the 90° spectra for the two projectiles are virtually identical in both shape and magnitude over the measured energy range, but at forward and backward angles they differ. For incident protons the preequilibrium component is stronger at the forward angle and weaker at the backward angle than for incident pions, and the slopes change much more with angle. In the low-energy evaporation part of the spectra there is little difference between the two projectiles. The slopes in the high-energy part of the ^{4}He spectra are independent of emission angle and pion energies, with a mean value of $T=13$ MeV.

Since the shapes of the fragment energy spectra for the other pion beams used in this study are similar to those shown in Figs. 3 and 4 for 160 MeV π^+, the dependence on pion charge and energy is most easily shown by integrating the energy spectra to obtain the differential cross section, $d\sigma/d\Omega$. The ^{3}He spectra were integrated from

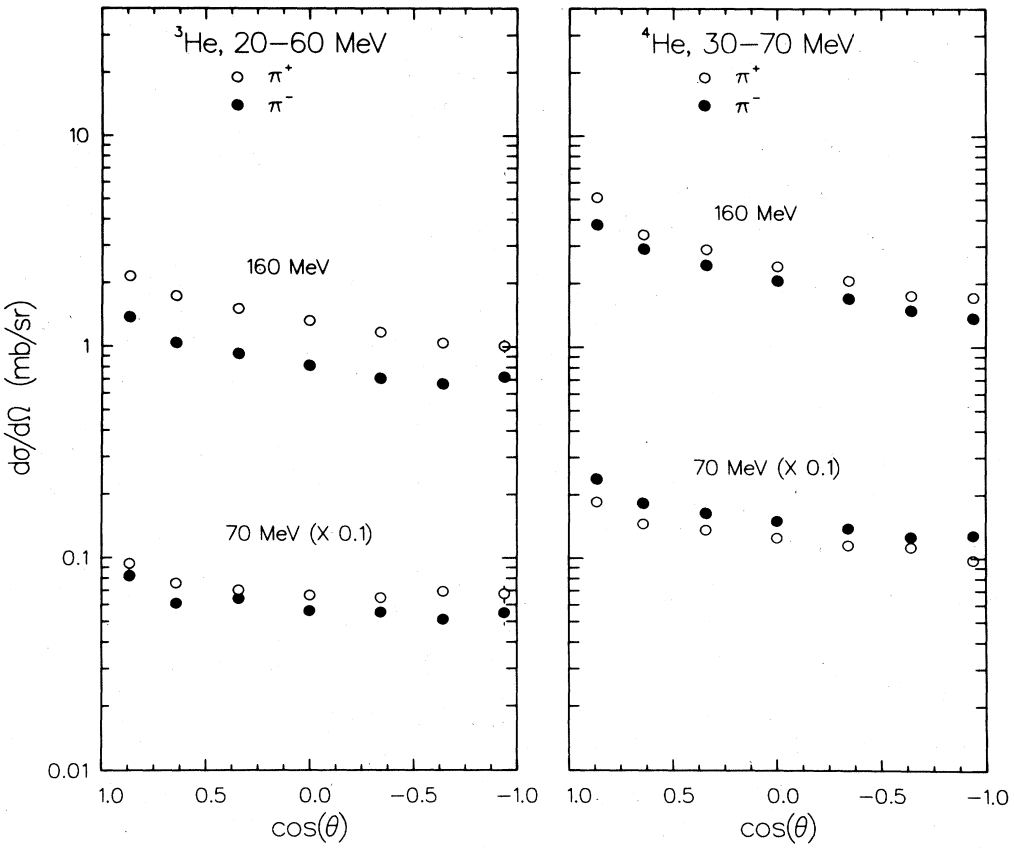

FIG. 5. Angular distributions of ^{3}He and ^{4}He for 160-MeV and 70-MeV π^+ and π^- interactions with Ag. The energy spectra were integrated from 20 to 60 MeV for ^{3}He and from 30 to 70 MeV for ^{4}He.

20 to 60 MeV and the ^{4}He spectra were integrated from 30 to 70 MeV, in order to exclude the evaporation contribution to the latter. Figure 5 shows the resulting cross sections in the form of angular distributions, as a function of the cosine of the emission angle. At an incident energy of 70 MeV, the ^{3}He cross sections are nearly independent of angle; only at the most forward angle is there a significant rise in cross section. The data for π^+ lie above those for π^-, but the angular dependence is similar. At the same incident energy the ^{4}He cross sections increase slowly toward forward angles, and again the values at 30° are above the trend of the data. The π^+/π^- ratio is reversed from that for ^{3}He, with larger π^- cross sections. At 160 MeV incident energy both fragments have forward-peaked angular distributions, and π^+/π^- ratios greater than unity. These ratios are uncertain to the extent of the precision of the absolute calibrations of the monitor cross sections, which was estimated[21] to be about 5%. The π^+ cross sections increase more with bombarding energy (a factor of 2 between 70 and 160 MeV) than do those for π^- (a factor of 1.4). These differences are due in part to the Coulomb effect, which decreases π^+ and increases π^- cross sections at the lower energy. A simple classical expression for this effect is

$$\sigma(\pi^{\pm}) \propto (1 \mp V/T_{\pi}) , \tag{1}$$

where $V = Ze^2/R$ is the Coulomb potential at the nuclear surface and T_{π} is the pion kinetic energy. In Table I are listed the π^+/π^- cross section ratios averaged over angle and these ratios corrected for the Coulomb effect, using a radius of $R = 1.2A^{1/3}$ fm. This correction accounts for most of the energy dependence of the cross section ratios. The last column of Table I gives the results of a simple statistical estimate of these ratios, based on a final-state interaction model and described in the following section.

TABLE I. π^+/π^- cross section ratios for fragment emission.

Fragment	T_{π} (MeV)	$\sigma(\pi^+)/\sigma(\pi^-)$	$\sigma(\pi^+)/\sigma(\pi^-)$ Corrected[a]	Calculated ratio
^{3}He	70	1.18	1.65	1.75
	160	1.62	1.88	
^{4}He	70	0.83	1.16	1.17
	160	1.20	1.39	

[a]Corrected for Coulomb effects using Eq. (1).

IV. DISCUSSION

The similarity between the fragment energy spectra from pion-induced reactions and the 90° spectra from proton-induced reactions suggests that similar mechanisms are involved, while the lack of a strong angular dependence of the former indicates a difference in the details of the mechanism. At the pion energies of this experiment the reaction cross section for medium-mass nuclei is made up of approximately equal contributions from true absorption and inelastic scattering, with a small amount of charge exchange.[23–25] On energetic grounds alone one expects pion absorption to be the dominant process responsible for fragment emission, since the total energy is thus available. The energetic nucleons formed as a result of the absorption then move through the nucleus and lead to fragment emission in the same way that a proton interacting with the target would. The difference in the two cases which affects the angular distribution is that the nucleons formed by absorption tend to move in opposite directions, so as to give a small resultant momentum, equal to that of the incident pion. The angular distribution of the final fragments is thus nearly isotropic, as a result of the near isotropy of the fast nucleons formed in the absorption. Pion scattering, on the other hand, is expected to contribute significantly to fragment emission only at the most forward angles, since sufficient energy can be transferred to a nucleon only as a result of backward scattering.

The fragment angular distributions shown in Fig. 5 are thus seen as an indication of the relative importance of pion absorption and scattering in energetic fragment emission. At 70-MeV incident energy the fragments are emitted nearly isotropically, with an increase in cross section occurring at the most forward angle. This is interpreted as evidence that the dominant process is indeed absorption, with pion-nucleon scattering contributing only at forward angles. At the higher incident energy of 160 MeV the angular distributions suggest an increased contribution from scattering processes. At still higher energies, as the kinetic energy becomes much larger than the pion rest mass, momentum conservation will focus the nucleons resulting from absorption to more forward angles, and thus lead to forward peaked fragment angular distributions, as observed for other projectiles. If absorption were "turned off," so that fast nucleons were formed only in scattering events, fragments would presumably be forward peaked even with a low momentum projectile as is observed in electron-induced reactions.[14–16]

The relative numbers of protons and neutrons produced by the absorption of π^+ and π^- should be the main influence on the π^+/π^- ratio of fragment yields. Qualitatively, π^+ absorption should favor emission of a proton-rich fragment such as ^{3}He, in agreement with the present results (Table I). More quantitatively, we may apply a final-state interaction model of fragment emission,[9–11] in which an energetic nucleon moving through the nucleus picks up additional nucleons to emerge as the observed fragment. If $P(\mathrm{p},F)$ and $P(\mathrm{n},F)$ are the relative probabilities of a proton and a neutron forming the fragment F, and $N(\pi^{\pm},\mathrm{p})$ and $N(\pi^{\pm},\mathrm{n})$ are the numbers of protons and neutrons formed in $\pi^{\pm}$ absorption, then the π^+/π^- ratio for fragment F is

$$\frac{\sigma(\pi^+,F)}{\sigma(\pi^-,F)}=\frac{N(\pi^+,\mathrm{p})P(\mathrm{p},F)+N(\pi^+,\mathrm{n})P(\mathrm{n},F)}{N(\pi^-,\mathrm{p})P(\mathrm{p},F)+N(\pi^-,\mathrm{n})P(\mathrm{n},F)} . \quad (2)$$

The values for N can be estimated by using experimental data on energetic proton yields from π^+ and π^- interactions on different targets.[26–28] For medium-mass targets the ratio of proton cross sections, corrected for the Coulomb effect, was found to be $\sigma(\pi^+,\mathrm{p})/\sigma(\pi^-,\mathrm{p})=4.5$ at pion energies of 100 and 160 MeV. From charge symmetry we assume that $N(\pi^+\mathrm{n})=N(\pi^-,\mathrm{p})=1/5.5$ and $N(\pi^-,\mathrm{n})=N(\pi^+,\mathrm{p})=4.5/5.5$. The values of P are given in terms of the numbers of protons and neutrons, Z and N, in the nucleus; for example, for $F=^3$He, $P(\mathrm{p},F)=2ZN/A^2$ and $P(\mathrm{n},F)=Z^2/A^2$. The calculated values of the π^+/π^- ratios using this simple picture are given in the last column of Table I; the agreement with the (corrected) experimental ratios is reasonable, within the uncertainties of the calibration.

The question of how many nucleons are involved in pion absorption has been addressed in recent publications.[26–31] Analysis of the energetic proton spectra from pion-nucleus reactions[27] in terms of isotropic emission from a moving source showed that such a source corresponded to the transfer of the pion momentum and total energy to about three nucleons for a ^{12}C target, increasing to 5–6 nucleons for a ^{181}Ta target. The ratio of 4.5 for proton yields from π^+ and π^- is much smaller than would be expected if two-nucleon absorption dominated.[28] Analysis of the two-proton coincidences in the $^{12}\mathrm{C}(\pi^+,2\mathrm{p})$ reaction led to the conclusion that the two-nucleon process accounted for less than 10% of the absorption cross sections.[29] Alternative explanations of these data have retained the conventional two-nucleon mechanism by including the effects of rescattering of the outgoing nucleons[30] and multiple scattering of the pion before absorption.[31] In any case, the evidence is that in medium-mass nuclei the pion momentum and total energy are somehow distributed among 4–5 nucleons following absorption.

The moving-source analysis which was used[27] to analyze the proton spectra has also been applied to spectra of light fragments from relativistic heavy-ion reactions[32] and medium-energy proton reactions.[5–7] The basis is a thermal or statistical model, which postulates isotropic emission of the energetic fragments from a moving, excited source. Such a hot localized region of the nucleus might be formed as a result of pion absorption, with the available energy spread over a small number of nucleons. In this analysis the data are expressed as a relativistically invariant cross section, $p^{-1}d^2\sigma/d\Omega\,dE$ as a function of momentum, and contours of the constant cross section are drawn on the plane defined by the coordinates $p_\perp/Mc$ and y, where $p_\perp$ is the fragment momentum component perpendicular to the beam direction, M is the fragment mass, and $y=\tanh^{-1}(\beta_\parallel)$ is the fragment rapidity. In this representation isotropic emission from a nonrelativistic source which is moving with rapidity y_0 is characterized by circular contours of constant cross section centered at $y=y_0$. In this way one can see to what extent the data are

consistent with this simple picture without assuming a specific form for the energy spectrum in the moving frame. The values of y_0 found for the proton spectra from pion interactions[27] were related to the number of nucleons, N, which absorbed the momentum and energy of the pion by the equation

$$y_0 = \tanh^{-1} \frac{p_\pi c}{E_\pi + N M_N c^2} , \quad (3)$$

where p_π and E_π are the momentum and total energy of the incident pion and M_N is the nucleon mass.

Applied to light fragment spectra[5–7,32] this analysis showed that while circular contours of constant invariant cross section in the $(y, p_\perp/Mc)$ plane did fit the data for all fragments measured, the value of y_0, the center of each circle, varied with contour level. In terms of the picture of fragment emission from a moving source, the source velocity, $\beta_s \approx y_0$, increased as a function of the fragment velocity in the moving frame, β_r, the radial velocity (i.e., the radius of a given contour). Furthermore, the relation between β_s and β_r was approximately linear and virtually identical for all fragments. These systematics were interpreted as indicating a distribution of excited sources recoiling with different velocities, with a correlation such that more highly excited (hotter) sources tend to have higher velocities. This would result in the observed correlation of velocities, since a hotter source would tend to emit more energetic fragments.

In analyzing the present fragment spectra in this way, the differential cross sections were converted to the invariant form and fitted to smooth curves as a function of fragment momentum. Sets of data points at constant cross section were interpolated from these curves and plotted on the $(y, p_\perp/Mc)$ plane. It was apparent from these plots that circular contours could fit the data well, with the exception of the 30° point, which in most cases lay at higher values of rapidity than the other points. This is a consequence of the larger cross sections at 30° seen in the angular distributions of Fig. 5. The point at 30° was therefore omitted from the least squares fit of the data to circles.

An example of such a plot for the ^{4}He spectra from 160 MeV π^+ reactions is shown in Fig. 6, where the deviations of the points at 30° from the fitted contours can be seen. The value of y_0 for each contour is indicated by a short vertical line, from which one can see that y_0, although small, increases with increasing fragment velocity. The small values of the source velocities compared to the fragment velocities are related to the small extent of anisotropy in the fragment angular distributions; as a consequence the source velocities obtained by this analysis have sizable uncertainties, especially for the ^{3}He spectra. Within these uncertainties the correlation between source velocity and fragment velocity was found to be similar for the two He isotopes, and to change with pion energy. This correlation is shown in Fig. 7, together with the curve representing the data for ^{4}He in 480-MeV proton reactions.[6] As discussed above, these curves are interpreted as indicating a distribution of sources, with the more energetic fragments being emitted from the faster moving sources. In terms of Eq. (3), this also implies a wide range for the number of nucleons, N, over which the energy and momentum of the pion are distributed. The largest values of β_s shown in Fig. 7 correspond to values of $N=27$ for 70 MeV pions and $N=21$ for 160 MeV pions, while the smallest values correspond to the entire nucleus participating. Although the source velocities derived from the 480-MeV proton data are much larger than for pions, the higher proton momentum results in similar values for N when Eq. (3) is applied.

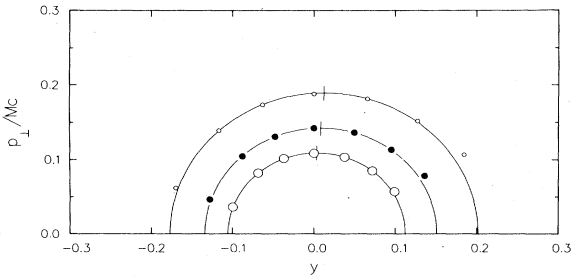

FIG. 6. Sets of data points of constant invariant cross section in the $(y, p_\perp/Mc)$ plane for ^{4}He from 160-MeV π^+ interactions with Ag. The curves are circles corresponding to isotropic emission from sources moving with rapidity y_0, the values of which are shown by vertical lines on each contour. The contour levels are at invariant cross section values of 2, 0.2, and 0.02 μb/[(MeV/c) (MeV sr)].

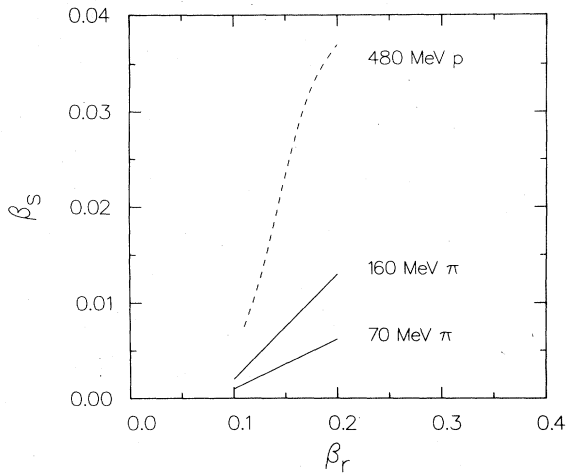

FIG. 7. Correlation between source velocity β_s and radial velocity β_r for ^{4}He from reactions of 70-MeV and 160-MeV $\pi^\pm$ and of 480-MeV protons with Ag.

V. SUMMARY

Energy spectra of ^{3}He and ^{4}He fragments emitted in the reactions of 70-MeV and 160-MeV π^+ and π^- mesons with Ag have been measured at seven laboratory angles between 30° and 160°. The ^{3}He energy spectra are all of the form of an exponentially decreasing cross section, $\exp(-E/T)$, with slope parameters averaging about 25 MeV. The ^{4}He spectra show evidence of two components, a low energy one attributed to statistical evaporation, and a high energy direct or preequilibrium part, with a slope

parameter T of about 13 MeV. These spectra are similar in shape and magnitude to the spectra for the same fragment observed at 90° in the reactions of 300—480 MeV protons with Ag. However, the strong variation with angle of these energy spectra, which is characteristic of the reactions of protons as well as other projectiles, is not observed for these pion reactions. Instead, there is little variation of either the shape or the magnitude of the spectra with angle. As a result, the fragment angular distribution are not strongly peaked in the forward direction, as is the case for other projectiles, and indeed at 70-MeV incident energy are nearly isotropic for ^{3}He.

It is concluded that pion absorption, in which the total energy of the pion is available for the reaction, is the dominant mechanism for fragment emission. It is the nucleons which have participated in the absorption and thus taken up this energy which then lead to fragment emission. These secondary nucleons will tend to move through the nucleus in opposite directions, because of the relatively low incident momentum, while secondary nucleons formed by scattering will move predominantly in the forward direction. Only at the most forward angles is there evidence for some contribution of pion scattering to fragment emission. The similarity of the fragment energy spectra to those observed at 90° in medium-energy proton reactions, together with the lack of a strong angular correlation, can thus be understood.

A single-scattering model has been proposed to account for light-fragment emission in reactions of medium-energy protons and electrons.[9—11] In this model the observed fragment is assumed to result from final-state interactions of the recoiling nucleon following an initial projectile-nucleon scattering, in which additional nucleons are picked up. The probability that a proton will pick up an additional proton and neutron to emerge as ^{3}He is approximately twice the probability that a neutron will pick up two protons (for a $N=Z$ nucleus). Because π^+ absorption yields more protons than does π^- absorption (by about a factor of 4), this results in a higher yield of ^{3}He from π^+ than from π^- reactions. The experimental cross sections, when corrected for the Coulomb effect, are consistent with this mechanism.

The data were also analyzed in terms of a statistical model, assuming isotropic emission of the fragments from an excited moving source. A correlation between the source velocities and the fragment velocities was found, which suggested that the higher energy fragments tend to be emitted from the faster moving sources. A similar relationship has been previously observed for fragments emitted in reactions of both relativistic heavy ions and medium-energy protons. If one equates the velocity of the source with the velocity of an assumed cluster of nucleons which has absorbed the total energy and momentum of the pion, the cluster sizes vary from about 20—30 nucleons to essentially the entire nucleus.

ACKNOWLEDGMENTS

We gratefully acknowledge the work of the LAMPF technical staff and operating crews for their help in carrying out this experiment. We especially wish to thank M. J. Leitch for assistance in tuning the beam and providing the muon telescope used in beam monitoring, and B. J. Dropesky and G. C. Giesler for assistance in counting the activity of the foil monitors. This research was supported by the Office of High Energy and Nuclear Physics, Division of Nuclear Physics, U.S. Department of Energy, under Contract Number W-31-109-ENG-38 and by the Natural Sciences Engineering Research Council of Canada.

[1]For a recent review, see D. H. Boal, in *Advances in Nuclear Physics,* edited by J. W. Negele and E. W. Vogt (Plenum, New York, to be published).

[2]J. R. Wu, C. C. Chang, and H. D. Holmgren, Phys. Rev. C **19**, 698 (1979).

[3]J. R. Wu, C. C. Chang, and H. D. Holmgren, Phys. Rev. C **19**, 370 (1979).

[4]J. R. Wu, C. C. Chang, and H. D. Holmgren, Phys. Rev. C **19**, 659 (1979).

[5]R. E. L. Green and R. G. Korteling, Phys. Rev. C **18**, 311 (1978).

[6]R. E. L. Green and R. G. Korteling, Phys. Rev. C **22**, 1594 (1980).

[7]R. E. L. Green, R. G. Korteling, and K. P. Jackson, Phys. Rev. C **29**, 1806 (1984).

[8]D. H. Boal and R. M. Woloshyn, Phys. Rev. C **20**, 1878 (1979).

[9]D. H. Boal, R. E. L. Green, R. G. Korteling, and M. Soroushian, Phys. Rev. C **23**, 2788 (1981).

[10]D. H. Boal, Phys. Rev. C **25**, 3068 (1982).

[11]D. H. Boal and M. Soroushian, Phys. Rev. C **25**, 1003 (1982).

[12]H. H. Gutbrod, A. Sandoval, P. J. Johansen, A. M. Poskanzer, J. Gosset, W. G. Meyer, G. D. Westfall, and R. Stock, Phys. Rev. Lett. **37**, 667 (1976).

[13]J. Gosset, H. H. Gutbrod, W. G. Meyer, A. M. Poskanzer, A. Sandoval, R. Stock, and G. D. Westfall, Phys. Rev. C **16**, 629 (1977).

[14]A. G. Flowers, A. C. Shotter, D. Branford, J. C. McGeorge, and R. O. Owens, Phys. Rev. Lett. **40**, 709 (1978).

[15]A. G. Flowers, D. Branford, J. C. McGeorge, A. C. Shotter, P. Thornley, C. H. Zimmerman, R. O. Owens, and J. S. Pringle, Phys. Rev. Lett. **43**, 323 (1979).

[16]A. G. Flowers, P. J. Thornley, I. Anthony, D. Branford, J. C. McGeorge, M. R. Sene, A. C. Shotter, and C. H. Zimmerman, Nucl. Phys. **A429**, 61 (1984).

[17]D. H. Boal and R. M. Woloshyn, Phys. Rev. C **23**, 1206 (1981).

[18]J. F. Amann, P. D. Barnes, M. Doss, S. A. Dytman, R. A. Eisenstein, J. Penkrot, and A. C. Thompson, Phys. Rev. Lett. **35**, 1066 (1975).

[19]A. Doron, A. Altman, D. Ashery, Y. Shamai, A. I. Yavin, J. Julien, Y. Cassagnou, H. E. Jackson, R. Legrain, A. Palmeri, and S. Barbarino, Phys. Rev. C **18**, 961 (1978).

[20]H. S. Pruys, R. Engfer, R. Hartmann, E. A. Hermes, H. P. Isaak, F. W. Schleputz, U. Sennhauser, W. Dey, K. Hess, H. J. Pfeiffer, H. K. Walter, and W. Hesselink, Nucl. Phys. **A352**, 388 (1981), and references therein.

[21]B. J. Dropesky, G. W. Butler, G. C. Giesler, C. J. Orth, and R. A. Williams, Phys. Rev. C **32**, 1305 (1985).

[22]A. G. Seamster, R. E. L. Green, and R. G. Korteling, Nucl. Instrum. Methods **145**, 583 (1977).
[23]K. Nakai, T. Kobayashi, T. Numao, T. A. Shibata, J. Chiba, and K. Masutani, Phys. Rev. Lett. **44**, 1446 (1980).
[24]D. Ashery, I. Navon, G. Azuelos, H. K. Walter, H. J. Pfeiffer, and F. W. Schleputz, Phys. Rev. C **23**, 2173 (1981).
[25]I. Navon, D. Ashery, J. Alster, G. Azuelos, B. M. Barnett, W. Gyles, R. R. Johnson, D. R. Gill, and T. G. Masterson, Phys. Rev. C **28**, 2548 (1983).
[26]H. E. Jackson, S. L. Tabor, K. E. Rehm, J. P. Schiffer, R. E. Segel, L. L. Rutledge, Jr., and M. A. Yates, Phys. Rev. Lett. **39**, 1601 (1977).
[27]R. D. McKeown, S. J. Sanders, J. P. Schiffer, H. E. Jackson, M. Paul, J. R. Specht, E. J. Stephenson, R. P. Redwine, and R. E. Segel, Phys. Rev. Lett. **44**, 1033 (1980).
[28]R. D. McKeown, S. J. Sanders, J. P. Schiffer, H. E. Jackson, M. Paul, J. R. Specht, E. J. Stephenson, R. P. Redwine, and R. E. Segel, Phys. Rev. C **24**, 211 (1981).
[29]A. Altman, E. Piasetzky, J. Lichtenstadt, A. I. Yavin, D. Ashery, R. J. Powers, W. Bertl, L. Felawka, H. K. Walter, R. G. Winter, and J. v. d. Pluym, Phys. Rev. Lett. **50**, 1187 (1983).
[30]K. G. R. Doss and W. R. Wharton, Phys. Rev. C **22**, 1219 (1980).
[31]V. Girija and D. S. Koltun, Phys. Rev. Lett. **52**, 1397 (1984); J. P. Schiffer, *ibid.* **53**, 736 (1984); V. Girija and D. S. Koltun, *ibid.* **53**, 737 (1984).
[32]P. B. Price and J. Stevenson, Phys. Lett. **78B**, 197 (1978).